results in Fig. 6, the angular distribution below 8 Mev, are consistent with this model.

The total cross section for charged particle emission was found to be 87 ± 22 mb, which may be compared with the results of Armstrong and Brolley.[25] Calculated values obtained by the method of Blatt and Weisskopf,[5] give 8.9 mb for a square well. This result suggests that the diffuse nuclear potential is probably a better approximation to the truth than the square well.

[25] A. H. Armstrong and J. E. Brolley, Jr., Phys. Rev. **99**, 330 (1955).

IV. ACKNOWLEDGMENTS

We wish to thank Dr. S. Wexler of the Argonne National Laboratory for filling our gas target, and Dr. L. Rayburn of the same laboratory for much help, especially for carrying out the positron annihilation count. We wish to thank Dr. K. Kikuchi of the University of Minnesota for assistance in the theoretical calculations. We also wish to thank the staff of the Northwestern University Nuclear Physics Research Laboratory for help in construction of the apparatus, and the Low-Energy Emulsion Group for help in track measurements and data analysis.

PHYSICAL REVIEW VOLUME 119, NUMBER 5 SEPTEMBER 1, 1960

Multiple Scattering Correction for Proton Ranges and the Evaluation of the *L*-Shell Correction and *I* Value for Aluminum

HANS BICHSEL* AND EDWIN A. UEHLING
University of Washington, Seattle, Washington
(Received April 14, 1960)

Multiple scattering corrections to proton range-energy measurements are discussed. Curves are plotted which give the fractional transmission of protons through a finite thickness of stopping material as a function of the initial proton energy and for various values of the ratio of the straggling and multiple scattering parameters. An application of these results to particular experimental situations shows that the Molière multiple scattering distribution gives a nearly correct representation of the experimental data on transmission and that a simple exponential distribution is not satisfactory. The case of straggling in gold is discussed in detail. Application of the results to the experimental range-energy relation in aluminum for protons of energy lying between 1 and 20 Mev is made. The experimental ranges can be described consistently with a mean excitation potential $I=163$ ev and with reasonable values of the *L*-shell binding energy correction.

I. INTRODUCTION

IN order to compare the results of range-energy measurements with the theory of stopping power, we must be able to make an accurate determination of a number of small quantities which appear as corrections in both the theory and the measurements. Failure to make a consistent application of such corrections in the past is partially responsible for the fact that stopping power relations based on a velocity-independent mean excitation potential have failed to predict correctly the measured ranges as a function of the energy of the penetrating particle. The discrepancies are small, but they are systematic and significant.

The most important correction to be made is in the stopping power relation itself. This is the correction for the binding energy of atomic electrons which has been discussed at some length by Walske.[1] Since, however, the present state of the theory of binding energy corrections is such that adjustable parameters should be introduced, a consistent application of binding energy corrections is hardly possible unless other required experimental corrections are made at the same time.

The most important of these other corrections is the multiple scattering correction. With the increasing accuracy of range-energy determinations it is of some importance that this correction be taken into account correctly. This will be the case even when the multiple scattering correction is of the same order as the error of measurement. The monotonic nature of the multiple scattering correction tends to remove a systematic trend in the discrepancy between theory and experiment. A more consistent application of the theory will then be possible. An immediate result of such a comparison of theory and experiment is a better determination of the mean excitation potential *I*.

We will be concerned here both with the method of determining the needed stopping power and range-energy corrections and with the application of these ideas in particular cases. The theory of the multiple scattering correction will be discussed in Sec. II. This section will contain also the results of numerical calculations; in particular, the transmission curves for protons of intermediate energy in several media. In Sec. III we make an application of these results to the

* Now at the University of Southern California, Los Angeles, California, where part of this work was done.

[1] M. C. Walske, Phys. Rev. **88**, 1283 (1952); **101**, 940 (1956).

transmission of 10-Mev protons in gold and attempt to establish the validity of the theory. Results of the comparison of theory and experiment for other materials and other energies are also given. Finally, in Sec. IV we make an application to the case of protons in aluminum and obtain a numerical value of I that is consistent with experimental data over a rather large range of proton energies, and experimental values for the L-shell correction.

II. MULTIPLE SCATTERING CORRECTION

As a monenergetic beam of protons (or other heavy charged particle) enters a foil of material, it will suffer degradation in energy and direction.[2] The energy degradation is described by the theory of stopping power and is caused mainly by collisions with the atomic electrons. The associated straggling in energy or range is approximately Gaussian in form and does not by itself make a contribution to the average path length. The change in direction at low and medium energies (i.e., up to about 100 Mev) is caused mainly by Coulomb scattering of the protons by nuclei. Since a large number of small-angle deflections take place along the path of the proton, the phenomenon is one of multiple scattering, for which accurate theories have been developed by Snyder and Scott and by Molière.[3] The multiple scattering leads to an additional distribution in path length for particles emerging from the foil. The nature of this distribution is such as to make all path lengths in the material greater than the foil thickness by an amount which depends on the magnitude of the straggling distribution as well as the multiple scattering distribution.

We are assisted in the evaluation of the multiple scattering contribution to path length by recognizing that it is the *median* range rather than the mean range which is obtained most directly from the transmission curve of a range-energy experiment such as that described in recent measurements.[4,5] An approximate evaluation may therefore be based on the calculation of a median path length in a foil of thickness t. A little consideration of the problem shows that there are contributions to the median path length which are of two kinds: the length of the smoothed-out median path which is described under the influence of the combined straggling and multiple scattering distributions; and an increment which represents the average difference between the actual path and the smoothed-out path.

In order to describe the contribution of the first kind, we begin in the usual way by considering that the total path length l is the sum of successive increments Δl_i; which can be written in terms of the angle Θ_i between the incident beam direction and the direction which the proton path has (or which we assign to it) in the ith segment.

$$l=\sum_i \Delta l_i=\sum_i \frac{\Delta l_i}{\cos\Theta_i}\cong\sum_i \Delta l_i\left(1+\frac{\Theta_i^2}{2}\right)$$

$$=t+\tfrac{1}{2}\sum_i \Theta_i^2\Delta l_i=t+\tfrac{1}{2}\int\Theta^2 dt.$$

Then the increment in path length (in this small-angle approximation) is

$$\Delta R=l-t=\tfrac{1}{2}\int\Theta^2 dt=\tfrac{1}{2}\int\Theta^2\frac{dE}{(-dE/dt)}, \tag{1}$$

where $(-dE/dt)$ is the stopping power as a function of proton energy in the foil. We now use the multiple scattering theory in the form given by Molière. This theory describes the distribution in angle for a particle which has traversed a distance t of the stopping medium and has lost the corresponding amount of energy. The distribution function is

$$f(\Theta)\Theta d\Theta=g(\vartheta)\vartheta d\vartheta, \tag{2}$$

where

$$g(\vartheta)=2\exp(-\vartheta^2)+f^{(1)}(\vartheta)/B+f^{(2)}(\vartheta)/B^2,$$

with

$$\vartheta^2=\Theta^2/\chi_c^2 B,$$

and

$$\chi_c^2=4\pi NZ(Z+1)z^2e^4\int_0^t\frac{dt}{p^2v^2}.$$

Also $f^{(1)}$ and $f^{(2)}$ are functions tabulated by Molière and B is defined by the relation

$$B-\ln B=b,$$

where

$$b=2\ln(\chi_c/\Theta_a)+1-2C.$$

C is Euler's constant, Θ_a is a minimum scattering angle which depends on the screening of the atomic field, and all other symbols have their usual meanings. Note that Θ is a laboratory angle and that ϑ is a reduced angle. To the extent that B is a constant for a particle traversing the foil and losing energy, the distribution in ϑ is independent of position in the foil. Since B is in fact nearly constant (for protons in gold, B lies between 8.5 and 10 for E lying between 1 and 10 Mev), one can describe a definite fraction dF of all particles as those lying in $d\vartheta$ by writing

$$dF=g(\vartheta)\vartheta d\vartheta, \tag{3}$$

where dF then is independent of distance into the foil. Similarly,

$$F=\int_0^\vartheta g(\vartheta)\vartheta d\vartheta \tag{4}$$

[2] E. Segrè, *Experimental Nuclear Physics* (John Wiley & Sons, Inc., New York, 1952), Vol. I, p. 166.
[3] See reference 2, p. 282, and the original papers listed in this reference.
[4] H. Bichsel, R. F. Mozley, and W. A. Aron, Phys. Rev. **105**, 1788 (1957).
[5] H. Bichsel, Phys. Rev. **112**, 1089 (1958).

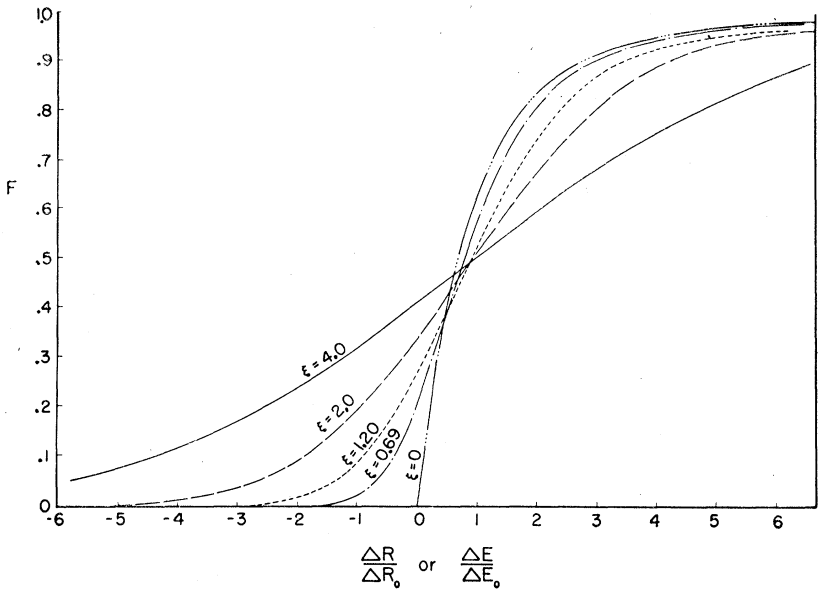

FIG. 1. Transmission curves for several values of $\xi=\Delta R_s/\Delta R_0$, the ratio of the energy loss straggling parameter and the multiple scattering parameter.

is a definite fraction F of all particles whose magnitude depends on the upper limit ϑ and is practically independent of position. We can now write the connection between ϑ and the increment in path length ΔR belonging to the particles of longest path length within the fraction F. This is

$$\Delta R=\tfrac{1}{2}\int\vartheta^2\frac{dE}{(-dE/dt)}=\tfrac{1}{2}\vartheta^2\int_{E_1}^{E_0}\frac{\chi_c^2BdE}{(-dE/dt)} \quad (5)$$
$$=\vartheta^2\Delta R_0,$$

where the integration along the path is extended from the initial energy E_0 to the emerging energy E_1 at ϑ and

$$\Delta R_0=\tfrac{1}{2}\int_{E_1}^{E_0}\frac{\chi_c^2BdE}{(-dE/dt)} \quad (6)$$

is a multiple scattering parameter depending on E_0, E_1 and the material but independent of ϑ. ΔR_0 is the fundamental quantity required for the determination of the multiple scattering correction. In the small-angle approximation which we are using, ΔR_0 diverges as E_1 approaches zero. However, only particles of energy greater than a certain minimum value are detected, and, consequently, the appropriate value of E_1 to use in the calculation of ΔR_0 is this minimum energy. This energy is between 5 and 20 kev in the experiments which will be described later. Since the minimum energy is only rather poorly known and since in addition the multiple scattering angle becomes rather large at these low energies, particularly in the heavier stopping media, we will need to consider the accuracy of the calculations with respect to the choice of E_1 and the validity of the comparison of calculated and experimental quantities in more detail later.

We can now write the multiple scattering distribution function in terms of the range ΔR. Since

$$\vartheta^2=\Delta R/\Delta R_0,$$
$$dF=g(\vartheta)\vartheta d\vartheta=g\left[\left(\frac{\Delta R}{\Delta R_0}\right)^{\frac{1}{2}}\right]\frac{d(\Delta R)}{2\Delta R_0},$$

or

$$dF=h(\Delta R)d(\Delta R), \quad (7)$$

where

$$h(\Delta R)=\frac{1}{2\Delta R_0}g\left[\left(\frac{\Delta R}{\Delta R_0}\right)^{\frac{1}{2}}\right] \quad (8)$$

is the multiple scattering distribution function in ΔR for smoothed-out paths in the foil. We will be interested in the fraction of particles whose increments in path length lie below a certain value ΔR. Thus

$$F(<\Delta R)=\int_0^{\Delta R}h(\Delta R)d(\Delta R). \quad (9)$$

Simple results are obtained in the approximation which neglects $f^{(1)}$ and $f^{(2)}$ of the Molière distribution. Then

$$h(\Delta R)=(1/\Delta R_0)e^{-\Delta R/\Delta R_0},$$
$$F(<\Delta R)=1-e^{-\Delta R/\Delta R_0},$$

and for the median path $[F(<\Delta R)=\frac{1}{2},\ \Delta R=\Delta R_{\frac{1}{2}}]$

$$\Delta R_{\frac{1}{2}}=\Delta R_0\ln 2.$$

These results for the smoothed-out path distribution are modified by the energy or range straggling. The straggling distribution for heavy particles is given by

$$p(R)dR=\frac{1}{(2\pi)^{\frac{1}{2}}\Delta R_s}\exp[-(R-R_0)^2/2(\Delta R_s)^2]dR. \quad (10)$$

Thus, from the straggling we obtain a distribution function in range ΔR directly. It is

$$dF=k(\Delta R)d(\Delta R), \tag{11}$$

where

$$k(\Delta R)=\frac{1}{(2\pi)^{\frac{1}{2}}\Delta R_s}\exp[-(\Delta R)^2/2(\Delta R_s)^2]. \tag{12}$$

Since both distributions are present simultaneously, the actual distribution in range is obtained as the folding of one distribution into the other. Thus, we now write

$$\begin{aligned} dF&=\int_0^\infty h(\Delta R')d(\Delta R')k(\Delta R-\Delta R')d(\Delta R)\\ &=d(\Delta R)\int_0^\infty h(x)k(\Delta R-x)dx\\ &=d(\Delta R)\int_{-\Delta R}^\infty h(\Delta R+x)k(-x)dx, \end{aligned} \tag{13}$$

$$F(<\Delta R)=\int_{-\infty}^{\Delta R}dy\int_0^\infty h(x)k(y-x)dx. \tag{14}$$

Then the increment in path length due to multiple scattering for the median particle, $\Delta R_{\frac{1}{2}}$, is determined by the relation

$$\tfrac{1}{2}=\int_{-\infty}^{\Delta R_{\frac{1}{2}}}dy\int_0^\infty h(x)k(y-x)dx. \tag{15}$$

If $F(<\Delta R)$ is expressed as a function of $\Delta R/\Delta R_0$ it depends in addition only on $\xi\equiv\Delta R_s/\Delta R_0$ representing the ratio of straggling and multiple scattering parameters. In the limit of $\xi\rightarrow\infty$ one has only straggling and $\Delta R_{\frac{1}{2}}/\Delta R_0\rightarrow 1$; i.e., $\Delta R_{\frac{1}{2}}\rightarrow 0$. In the limit of $\xi\rightarrow 0$ one has only multiple scattering and $\Delta R_{\frac{1}{2}}/\Delta R_0\rightarrow$ a finite value which is ln2 for the case of $f^{(1)}=f^{(2)}=0$ but is slightly less than ln2 for the actual Molière distribution. The family of curves $F(<\Delta R)$ as a function of $\Delta R/\Delta R_0$ for various values of ξ must be obtained by numerical integration. The calculated curves for $\xi=0$, 0.69, 1.2, 2.0, and 4.0 are shown in Fig. 1. As will be shown later the values of $\xi=0.69$, 1.2, 2.0, and 4.0 are approximately correct for protons in Au, Ag, Cu, and Al, respectively, at about 10 Mev. A useful numerical tabulation of the data from which the curves of Fig. 1 are plotted is given in Table I.

In order to display the difference between the Molière and a simple exponential distribution the curves of Fig. 2 are plotted. These curves are for $\xi=0$ and for the two cases of $B=10$ (as in Fig. 1) and $B=\infty$ (exponential distribution). The difference in shape and position of crossing the $F=0.5$ line are evident. These differences decrease as ξ increases. However, they are still important at finite values of ξ as we shall see when the comparisons with experimental data are made.

We are now ready to describe the first of the two main contributions to the path length of the median particle. This path length exceeds the thickness of the foil by the amount $\Delta R_{\frac{1}{2}}$ defined by Eq. (15). The numerical value of $\Delta R_{\frac{1}{2}}/\Delta R_0$ may be read directly from

TABLE I. Theoretical straggling distribution: fractional transmission F as a function of energy $\Delta E/\Delta E_0$ for several values of $\xi=\Delta R_s/\Delta R_0$ and for $B=10$, where ΔR_s is the energy loss straggling parameter and ΔR_0 is the multiple scattering parameter.

$\Delta R/\Delta R_0$ or $\Delta E/\Delta E_0$	ξ 0	0.69	1.20	2.0	4.0
−6.0				0.001	
−5.8				0.001	0.052
−5.6				0.001	
−5.4				0.002	0.064
−5.2				0.003	
−5.0				0.003	0.077
−4.8				0.004	
−4.6				0.005	0.092
−4.4				0.007	
−4.2				0.009	0.109
−4.0				0.012	
−3.8				0.015	0.128
−3.6				0.018	
−3.4				0.023	0.149
−3.2				0.029	
−3.0			0.002	0.036	0.173
−2.8			0.003	0.044	
−2.6			0.005	0.053	0.199
−2.4			0.008	0.064	
−2.2			0.012	0.077	0.227
−2.0			0.018	0.092	
−1.8			0.026	0.108	0.258
−1.6		0.002	0.037	0.126	
−1.4		0.006	0.050	0.146	0.289
−1.2		0.012	0.068	0.169	
−1.0		0.022	0.090	0.193	0.323
−0.8		0.039	0.118	0.220	
−0.6		0.064	0.149	0.248	0.358
−0.4		0.101	0.185	0.278	
−0.2		0.149	0.227	0.309	0.394
0.0	0	0.208	0.272	0.342	
0.2	0.190	0.276	0.321	0.376	0.432
0.4	0.340	0.350	0.372	0.411	
0.6	0.459	0.428	0.424	0.446	0.468
0.8	0.554	0.504	0.477	0.480	
1.0	0.630	0.577	0.530	0.515	0.506
1.2	0.691	0.638	0.579	0.551	
1.4	0.742	0.693	0.627	0.584	0.544
1.6	0.781	0.740	0.672	0.618	
1.8	0.814	0.780	0.712	0.650	0.580
2.0	0.840	0.814	0.748	0.680	
2.2	0.863	0.840	0.782	0.709	0.616
2.4	0.889	0.861	0.810	0.736	
2.6	0.896	0.880	0.836	0 762	0.651
2.8	0.910	0.896	0.856	0.786	
3.0	0.920	0.909	0.875		0.685
3.2	0.928	0.921	0.890	0.832	
3.4	0.936	0.928	0.903		0.716
3.6	0.943	0.938		0.866	
3.8	0.949		0.923		0.746
4.0	0.954	0.949		0.894	
4.2			0.937		0.776
4.4		0.957		0.915	
4.6			0.948		0.801
4.8		0.962		0.933	
5.0	0.970		0.954		0.823
5.2		0.968		0.945	
5.4			0.958		0.846
5.6		0.972		0.956	
5.8			0.963		0.865
6.0	0.980	0.976		0.963	
10.0	0.999	...	...	...	0.967

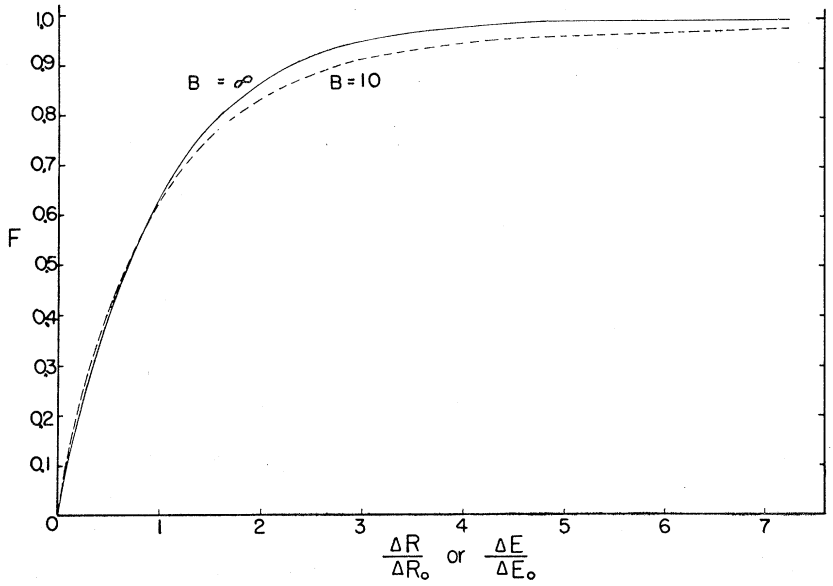

FIG. 2. Transmission curves for $\xi=0$ (multiple scattering contribution of the first kind only) with and without the Molière correction terms.

the curves of Fig. 1. Let us denote $q\equiv\Delta R_{\frac{1}{2}}/\Delta R_0$. This quantity is the value of $\Delta R/\Delta R_0$ at the point where the curve crosses the $F=0.5$ line. Numerical values of q for various values of ξ obtained in this way are given in Table II.

The data of Table II will be useful in the subsequent analysis of the range-energy measurements. At that time it will be useful also to compare values of ΔR_0 which will be obtained from the measurements with values calculated from Eq. (6). Table III lists the theoretical values of ΔR_0 as a function of proton energy for various materials.[6] For the purpose of these calculations E_1 is taken to be $0.01E_0$. Two considerations of importance in connection with these calculations of ΔR_0 are: the extent to which the small-angle approximation is fulfilled in these calculations; and the sensitivity of ΔR_0 to the choice of E_1. Relevant numerical data on these points are given in Tables IV and V. Table IV gives values of the square of the normal scattering angle $\Theta_0=\chi_c\sqrt{B}$ for various stopping media and various incident energies after a foil has been traversed and all but 20-kev energy has been lost. One observes that for the case of the heavy elements this angle is large and the small-angle approximation cannot be regarded as valid. However, Table V shows that ΔR_0 does not depend sensitively on the choice of E_1 for values of E_1 which are appropriate in our experiments. This table gives the dependence of the calculated ΔR_0 on E_1 for $E_0=10$ Mev in the case of a heavy element; namely, gold. One observes that ΔR_0 varies approximately linearly with E_1 over the range 100 kev $\lesssim E_1\lesssim 1$ Mev (which includes the maximum in the stopping power curve) and that the increase of ΔR_0 with decreasing E_1 below 100 kev is only slightly more rapid down to about 10 kev. At 10 kev ΔR_0 is less than 15% greater than the value obtained from an extrapolation of the linear relation. Since the experimental values of E_1 are of the order of 10 kev, we do not believe that our calculated values of ΔR_0 should be expected to differ very much from the experimental values, even in the case of gold.

TABLE II. Values of $q=\Delta R_{\frac{1}{2}}/\Delta R_0$ as a function of ξ with $B=10$, where q is the relative displacement of the straggling curve due to the influence of multiple scattering and coming from contributions of the first kind and $\xi=\Delta R_s/\Delta R_0$; the error is estimated from uncertainties in the numerical integration.

ξ	q	
0	0.684	(0.693 for $B=\infty$)
0.3	0.71	±0.03
0.6	0.79	
1.0	0.86	
1.5	0.88	
2.0	0.91	
4.0	0.96	±0.03
∞	1.00	

[6] Additional tabulations analogous to Tables I and V may be obtained from the first author.

In order to calculate the second contribution to the path length of the median particle, it is sufficient to use a simple exponential distribution. Also, it is convenient to use projected angles Θ_x and Θ_y rather than the polar angle Θ. Then for any given specification of emitted particle we have from Eq. (1)

$$\Delta R=\tfrac{1}{2}\int_0^t\Theta^2(t')dt',$$

$$\langle\Delta R\rangle_{\rm av}=\tfrac{1}{2}\int_0^t\langle\Theta^2\rangle_{\rm av}dt'=\tfrac{1}{2}\int_0^t\langle(\Theta_x^2+\Theta_y^2)\rangle_{\rm av}dt'$$

$$=\int_0^t\langle\Theta_x^2\rangle_{\rm av}dt'.$$

In order to carry out the desired calculation, we need to know the distribution in x and Θ_x at t'. This is[7]

$$F(t,x,\Theta_x)dxd\Theta_x = \frac{\sqrt{3}\,w^2}{2\pi\,t^2}\exp\left[-w^2\left(\frac{\Theta_x^2}{t}-\frac{3x\Theta_x}{t^2}+\frac{3x^2}{t^3}\right)\right]dxd\Theta_x,$$

from which the distribution in Θ_x alone is

$$G(t,\Theta_x)d\Theta_x=\frac{\sqrt{3}\,w^2}{2\pi\,t^2}d\Theta_x\int_{-\infty}^{\infty}\times\exp\left[-w^2\left(\frac{\Theta_x^2}{t}-\frac{3x\Theta_x}{t^2}+\frac{3x^2}{t^3}\right)\right]dx$$
$$=\frac{w}{2(\pi t)^{\frac{1}{2}}}\exp(-w^2\Theta_x^2/4t)d\Theta_x,$$

TABLE III. Theoretical values of ΔR_0 as a function of proton energy for several elements. The lower limit E_1 of the integral in Eq. (6) is taken to be 0.01 E_0.

E (Mev)	ΔR_0 (mg cm^{-2}) Al	Ni	Cu	Ag	Au
1	0.029	0.12		0.30	
1.5	0.046	0.17		0.43	
2	0.064	0.24		0.59	
3	0.10	0.36		0.89	
4	0.15	0.50		1.21	
6	0.26	0.84	0.94	1.97	5.5
8	0.40				7.7
10	0.56	1.74	1.88	3.9	10.3
12	0.74				13.1
14	0.95	2.88		6.3	
16	1.17	3.54			19.4
18	1.42	4.24	4.47	9.1	22.8
20	1.67	5.00			26.4
25	2.40	7.08		14.9	
30	3.23	9.43		19.7	46.9
34	3.95				56.1

and w is defined by the relation

$$\langle\Theta_x^2\rangle_{\rm av}=\int_{-\infty}^{\infty}G(t,\Theta_x)\Theta_x^2d\Theta_x=\frac{2t}{w^2}.$$

The distribution $G(t,\Theta_x)d\Theta_x$ has been used[8] to calculate $\langle\Delta R\rangle_{\rm av}$ for the two cases:

(*a*) All particles are detected irrespective of their position and angle of emergence after traversing a thickness t of the material.

(*b*) All particles emitted with $\Theta_x=\Theta_y=0$ and irrespective of position are detected.

The results of this calculation are $\langle\Delta R\rangle_{\rm av}=t^2/w^2$ in case (*a*) and $\langle\Delta R\rangle_{\rm av}=t^2/3w^2$ in case (*b*). We may now use the distribution function $F(t,x,\Theta_x)dxd\Theta_x$ in order to extend the calculation to two other cases of interest:

[7] B. Rossi and K. Greisen, Revs. Modern Phys. **13**, 240 (1941).
[8] C. N. Yang, Phys. Rev. **84**, 599 (1951).

TABLE IV. Calculated values of $\Theta_0^2=\chi_c^2B$ at $E_1=20$ kev for various values of the incident proton energy E_0 and for several stopping media; Θ_0 is the "normal" scattering angle in radians.

Stopping medium	E_0 in Mev 6	10	18	30
Al	0.248	0.255	0.264	0.271
Cu	0.75	0.77	0.79	···
Ag	1.26	1.29	1.33	1.36
Au	3.83	3.90	3.97	4.02

(*c*) Particles are detected if they emerge at $x=y=0$ and irrespective of angle.

(*d*) Particles are detected only if they emerge at $x=y=0$ and with $\Theta_x=\Theta_y=0$.

The results of this calculation are $\langle\Delta R\rangle_{\rm av}=t^2/5w^2$ in case (*c*) and $\langle\Delta R\rangle_{\rm av}=2t^2/15w^2$ in case (*d*).

The last case is of particular interest for our purpose. The smoothed-out path length for these particles is the thickness t of the material. Actually their path length exceeds t because of multiple scattering events which combine in such a way as to keep the particle near the smoothed-out curve and moving in the forward direction. The increase in path length is $2t^2/15w^2$. If the associated distribution in ΔR for all particles were precisely as given by Eq. (8), the ΔR of this equation would read $\Delta R-2t^2/15w^2$ instead of ΔR; or, in the notation of Yang[9] the distribution would start at $v=2w^2\Delta R/t^2=4/15$. The distributions plotted by Yang do in fact have their maximum rate of rise at a value of v close to $v=4/15\cong0.27$.

Energy loss in the foil can now be included in this calculation by noting that from Eq. (5)

$$\Delta R=\vartheta^2\Delta R_0$$

and consequently for all emerging particles

$$\langle\Delta R\rangle_{\rm av}=\Delta R_0,$$

since $\langle\vartheta^2\rangle_{\rm av}=1$ in the approximation we are using. Thus, by comparing the results of the calculation for the cases (*a*) and (*d*) we obtain for particles emerging

TABLE V. Calculated values of ΔR_0 as a function of the lower limit E_1 for protons in Au with $E_0=10$ Mev; values of $\Theta_0^2=\chi_c^2B$ are included.

E_1 (Mev)	Θ_0^2 (radians^2)	ΔR_0 (mg cm^{-2})	E_1 (Mev)	Θ_0^2 (radians^2)	ΔR_0 (mg cm^{-2})
6	0.039	1.50	0.4	0.436	9.48
4	0.077	3.51	0.3	0.507	9.70
3	0.116	4.87	0.2	0.623	9.95
2	0.157	6.45	0.1	0.93	10.28
1	0.247	8.22	0.08	1.079	10.37
0.9	0.273	8.42	0.06	1.331	10.50
0.8	0.294	8.62	0.04	1.903	10.70
0.7	0.318	8.83	0.03	2.524	10.86
0.6	0.348	9.04	0.02	3.898	11.14
0.5	0.387	9.26	0.01	8.826	11.82

[9] See reference 8, Fig. 1 and the text.

at $x=y=0$ with $\Theta_x=\Theta_y=0$ the result

$$\langle\Delta R\rangle_{\text{av}}=2\Delta R_0/15.$$

This is the second contribution to the multiple scattering correction.

Adding the two contributions we write the following expression for the path length of the median particle:

$$\begin{aligned}R&=t+\Delta R_{\frac{1}{2}}+2\Delta R_0/15\\&=t+(q+2/15)\Delta R_0.\end{aligned}\tag{16}$$

III. EXPERIMENTAL DETERMINATION OF THE MULTIPLE SCATTERING AND STRAGGLING PARAMETERS

In order to make comparisons with experiment it is convenient to regard all distributions, e.g., $F(<\Delta R)$, as functions of $\Delta E/\Delta E_0$ rather than $\Delta R/\Delta R_0$. This is possible since the lowest energy E_1 of detected particles is held constant during the measurements, and consequently an increase in $F(<\Delta R)$ is due solely to an increase ΔE in the incident energy where

$$\Delta E=\Delta R(-dE/dt)_{E=E_0}.$$

Therefore, the abscissa of Fig. 1 and the left-hand column of Table I can be regarded as values of $\Delta E/\Delta E_0$ as well as of $\Delta R/\Delta R_0$. The distribution $F(<\Delta E)$ thus represents the fraction of particles emerging from the foil which have an energy E_1 or greater as a function of the incident energy $E_0+\Delta E$.

It will be shown that one obtains a satisfactory comparison of theoretical and measured distributions only if one uses the full Molière multiple scattering function as described above. In principle we can determine ξ from a comparison of the experimental and theoretical distributions, ΔE_0 (and consequently ΔR_0) from the slope of F as a function of $\Delta E/\Delta E_0$, ΔR_s from ξ and ΔR_0, and finally, q from ξ and Table II. In practice the procedure may be varied somewhat as described in specific cases below. Checks on the theoretical calculations are to be found in the comparison of calculated and experimental distributions and in the comparison of calculated and experimental values of ΔR_s and ΔR_0.

Since q is determined by this procedure, the first of the two contributions to the excess path length as described in Eq. (16) is obtained. The second contribution is merely $2\Delta R_0/15$, and this is also obtained from the above procedure which determines ΔR_0. We do not have any independent experimental checks on this second contribution. However, it plays a role in the subsequent determination of the mean excitation potential I.

A typical measured distribution of the kind in which we are now interested is shown in Fig. 6 of reference 4. In order to make a comparison of theory and experiment we proceed as follows: Consider a set of values of the fractional transmission F. From the experimental data read off the corresponding values of the incident energy E. From the theoretical curve for a given ξ such as in Fig. 1, read off the corresponding values of $\Delta E/\Delta E_0$. Plot $\Delta E/\Delta E_0$ as a function of the measured E. If the theory is correct and the value of ξ has been properly chosen, the resulting curve will be a straight line. Thus ξ is determined.

Subsequent steps in the evaluation of parameters are as follows:

(*a*) From the straight line plot of $\Delta E/\Delta E_0$ versus the measured E, obtain ΔE_0 as the interval on the energy axis corresponding to a change in $\Delta E/\Delta E_0$ equal to 1.

(*b*) From $\xi=\Delta E_s/\Delta E_0$ and ΔE_0, obtain ΔE_s. Then, from ΔE_0 and ΔE_s, obtain ΔR_0 and ΔR_s by using tabulated values of the stopping power at the incident

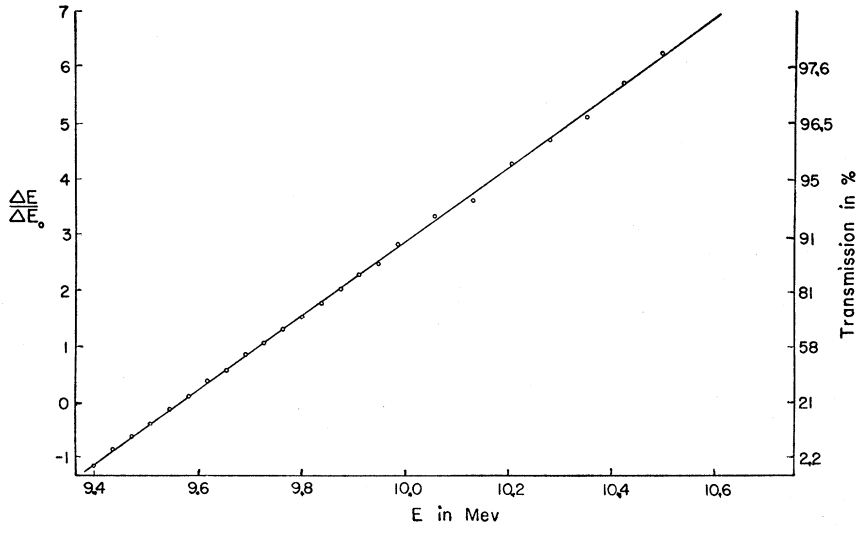

FIG. 3. Experimental transmission curve for 10-Mev protons in Au. Best fit is with $\xi=0.69$. The scale of ordinates on the right gives the actual percentage of transmitted protons (compare with Table I).

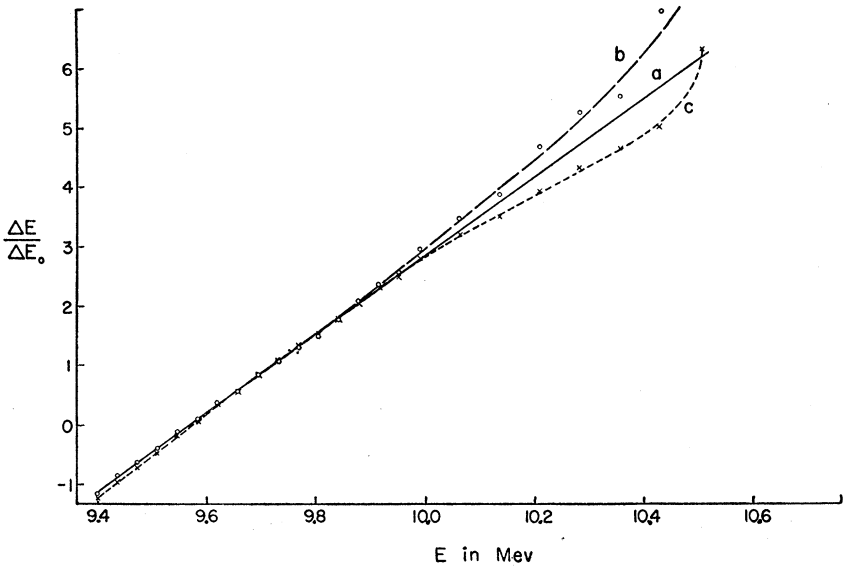

FIG. 4. Experimental transmission curves for 10-Mev protons in Au in which: curve a is the same as in Fig. (3) with $\xi=0.69$; curve b is similar except that all transmission values have been multiplied by 1.007; curve c is similar except that $\xi=0.775$ instead of $\xi=0.69$.

energy; i.e.,

$$\Delta R_0=\frac{\Delta E_0}{(-dE/dt)_{E=E_0}},$$

$$\Delta R_s=\frac{\Delta E_s}{(-dE/dt)_{E=E_0}}.$$

(c) From the tabulation of $q=\Delta R_{\frac{1}{2}}/\Delta R_0$ versus ξ as given in Table II, obtain $\Delta R_{\frac{1}{2}}=q\Delta R_0$.

(d) Use Eq. (16) to obtain the actual range of the median particle.

As an example let us consider the case of 10-Mev protons in gold. Figure 3 shows the plot of $\Delta E/\Delta E_0$ versus the measured energy E for the case of $\xi=0.69$. A straight line is obtained. In order to check the sensitivity of the procedure and the possible uniqueness of the results we consider in turn each of the following factors:

(a) In the experiment some of the protons will undergo nuclear reactions and will disappear from the beam. For 10-Mev protons in gold, this loss of protons may be as much as 1%. Consequently, there is some ambiguity in the normalization of the experimental distribution curve. Also, the method of calculation which involves the use of only a limited number of points of the two distribution functions h and k introduces some errors of normalization as is indicated by the failure of F to be equal to 1.000 for the largest value of $\Delta E/\Delta E_0$ in Table I. This error is probably less than 2%. However, the consequences of different normalizations need to be determined.

(b) A check of the theory, and a determination of ξ, is presumably achieved when a straight-line plot such as is illustrated in Fig. 3 is obtained. We wish to know how sensitive to the choice of ξ this procedure is.

(c) An example of the difference between the full Molière and a simple exponential multiple scattering distribution was illustrated in Fig. 2. A test of the possibility of describing the experimental transmission curve without use of the full Molière distribution should also be made.

The first two points are illustrated in Fig. 4. The straight line curve (a) in this figure is a replot of the curve in Fig. 3 for $\xi=0.69$. A second curve (b) is obtained in precisely the same way except that the experimental transmission curve was normalized to a value 0.7% lower than before. A third curve (c) is plotted in which the only change is that a theoretical transmission curve with $\xi=0.775$ rather than 0.69 was used. It is clear that the procedure is sensitive to both of these factors and that for energies as low as 10 Mev the measured transmission without change in normalization should be used.

The importance of using the full Molière multiple scattering function is illustrated in Fig. 5. The straight-line curve (a) is again the curve of Fig. 3. The other curve (b) is obtained in an analogous procedure in which however numerical values of $F(<\Delta R)$ in Eq. (14) are obtained using a simple exponential rather than the full Molière function. One observes that the theoretical distribution based on the simple exponential function deviates considerably from the experimental distribution and that this deviation is in the expected direction (more protons appearing at higher energies, corresponding to the larger angles). The pure exponential is thus not a good representation of the multiple scattering.[10]

The procedure outlined has been carried through for

[10] For an earlier confirmation of this conclusion for the case of heavy particles, based however on a measurement of the distribution in angle, see H. Bichsel, Phys. Rev. **112**, 182 (1958).

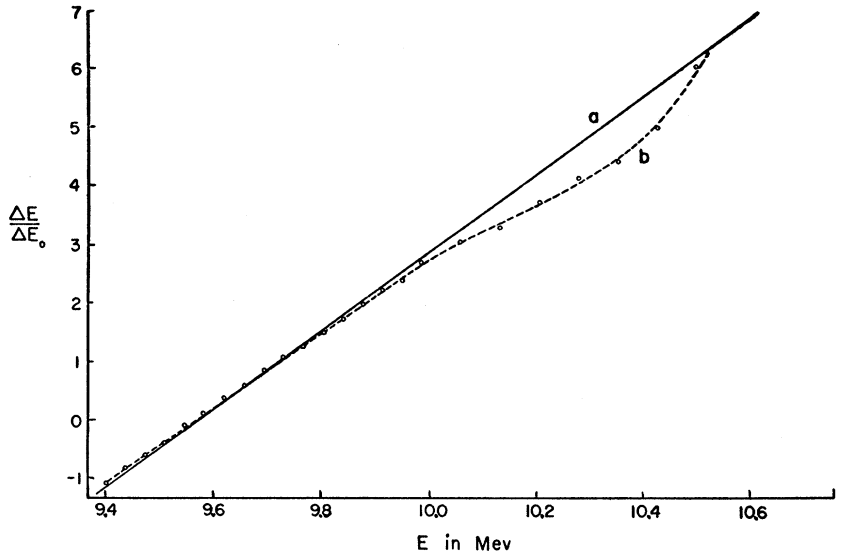

FIG. 5. Experimental transmission curves for 10-Mev protons in Au in which: curve a is again the same as in Fig. (3) with $\xi=0.69$; curve b is similar except that it is obtained with neglect of the Molière correction terms ($B=\infty$ instead of $B=10$).

Ag and Au. The results for proton energies of 10 and 18 Mev are given in Tables VI and VII. Values of ξ, ΔR_0, and ΔR_s determined in this way are to be found in columns 2, 3, and 6. Theoretical values of ΔR_0 listed in column 4 are calculated from Eq. (6) for the particular energy of an experiment rather than taken from Table III. Theoretical values of ΔR_s listed in column 7 are obtained from calculations of Millburn and Schecter.[11] Values of ξ and ΔR_0 (experimental) are not quoted in Tables VI and VII for Al and Cu. This is because these parameters are not so reliably determined by our procedure for the lighter elements as they are for the heavier elements, since the contribution of the multiple scattering to the straggling width is much less than the contribution of energy loss straggling. This does not prevent us, however, from making a reliable determination of ΔR_s, and in addition the value of ξ and ΔR_0 can at least be estimated. Our procedure for the determination of ΔR_s is as follows. For each of several values of ξ which are approximately correct for the element and the energy under consideration a value of ΔR_0 is obtained according to the procedure described above for a single ξ. Thus, one obtains pairs of numbers (ξ and ΔR_0) whose product $\Delta R_s=\xi\Delta R_0$ is observed to be very nearly a constant. This is not surprising since we are here considering cases of $\xi>1$ and for such cases the influence of the multiple scattering on the total straggling is small. The parameter ξ is itself not well determined since it may be permitted to vary over a rather wide range without altering the experimental distribution appreciably. Thus, for Al at 6 Mev we find practically no difference in the distribution for ξ anywhere in the range of 2.8 to 4.0. But ΔR_s is well determined at a value of 1.12 ± 0.03 mg cm^{-2}. Columns 5 and 8 give the ratios of experimentally and theoretically determined quantities. The agreement is probably better than we should have expected in view of the failure of the small-angle approximation as described previously (Sec. II), however much this failure may be minimized because the lowest detectable energy in the experiments lies sufficiently high so that the calculated and measured ΔR_0 are not strongly dependent on it.

[11] See Tables 8c-7 and 8c-5, in *American Institute of Physics Handbook* (McGraw-Hill Book Company, New York, 1957). R. M. Sternheimer, Phys. Rev. **117**, 485 (1960), gives values for R_s (theoretical) about 20% higher, agreeing quite closely with the values calculated in reference 4.

IV. I VALUE AND L-SHELL CORRECTION FOR ALUMINUM

The measured range corrected for multiple scattering as described in previous sections is to be compared with the theoretical range given by

$$R(E_0)=R(\epsilon)+\int_{\epsilon}^{E_0}\frac{dE}{(-dE/dt)}, \tag{17}$$

where $(-dE/dt)$ is the stopping power and ϵ is a lower limit in the energy above which the theoretical expression for stopping power can be regarded as valid and an accurate value of $R(\epsilon)$ can be assigned on the basis of measurements. The stopping power is computed from the expression

$$-\frac{1}{\rho}\frac{dE}{dt}=\frac{K(v)}{A}[Z(f(v)-\ln I)-\sum_i C_i], \tag{18}$$

where Z, A, and ρ are the atomic number, atomic mass and density of the stopping medium, I is the mean excitation potential, C_i are the shell corrections for

TABLE VI. Straggling parameters at 10 Mev (unless otherwise noted) for various stopping media together with an experimentally determined value of ξ for Ag and Au.

Stopping medium	ξ	ΔR_0 in mg cm^{-2} Exp.	Theory	Ratio	ΔR_s in mg cm^{-2} Exp.	Theory	Ratio
Al (6.15 Mev)	...	...	0.27	...	1.12±0.03	1.20	0.93
Cu	...	...	1.85	...	3.3 ±0.1	3.44	0.96
Ag	1.08±0.03	3.6±0.1	3.8	0.95	4.0 ±0.1	4.21	0.95
Au (9.7 Mev)	0.68±0.02	8.3±0.2	9.4	0.88	5.6 ±0.2	5.80	0.97

TABLE VII. Straggling parameters at 18 Mev (unless otherwise noted) for various stopping media together with an experimentally determined value of ξ for Ag and Au.

Stopping medium	ξ	ΔR_0 in mg cm^{-2} Exp.	Theory	Ratio	ΔR_s in mg cm^{-2} Exp.	Theory	Ratio
Al	...	...	1.41	...	6.4 ±0.2	6.4	1.00
Cu	...	...	4.4	...	8.45±0.03	8.5	1.00
Ag	1.12±0.02	8.7±0.2	8.9	0.98	9.8 ±0.2	10.3	0.95
Au (17.5 Mev)	0.70	20.0	21.0	0.95	14.0 ±0.5	13.7	1.02

binding energy and

$$K(v)=\frac{4\pi N_0 e^4}{mv^2}=\frac{4\pi N_0 r_0^2 mc^2}{\beta^2},$$

$$f(v)=\ln\frac{2mc^2\beta^2}{1-\beta^2}-\beta^2,$$

where N_0 is Avogadro's Number, m is the electron mass, and $\beta=v/c$.

In order to calculate $R(E_0)$ from Eq. (17) a value of I as well as binding energy corrections must be assigned. The function $R(E_0)$ obtained in this way is then compared with $R(E_0)$ as obtained from the measurements through Eq. (16). These two methods of obtaining $R(E_0)$ should agree over as large a range of variation of E_0 as possible for a single choice of I, $R(\epsilon)$, and the parameters which are used to fix the various shell corrections.

The application to aluminum is of interest because this stopping medium has been studied so extensively. In this case there are K- and L-shell corrections to be made and an M-shell correction which may be neglected. In order to reduce the number of free parameters we will assume that the K-shell correction as calculated by Walske[1] is correct. In order to fix the L-shell correction we make two assumptions:

(*a*) The ratio of the energy at which the maximum in C_i occurs and the energy of the i-shell electrons is independent of i; in particular, it is the same for L and K electrons. For protons in aluminum, C_K has its maximum at 4.6 Mev. Since the ionization potential of K-shell electrons[12] is 1560 ev, the ratio in question is 2900. Applying this ratio to an ionization energy of 72 ev for $2p$ electrons and 116 ev for $2s$ electrons, one finds that maxima in the L-shell correction occur at 0.21 and 0.34 Mev. The corresponding maxima in the M-shell correction would occur at energies of the order of 30 kev; consequently M-shell corrections are neglected completely, especially since only 3 M-shell electrons are present.

(*b*) At large proton energies $C_L\sim\kappa/E$, where κ is a constant and E is the energy. If the lower limit of

TABLE VIII. Calculated pathlength in Al for protons of energy E as a function of the mean excitation potential I and the constant κ of the L-shell correction. c_K according to Walske.

E (Mev)	Path length (mg cm^{-2})	I=166 κ=0	164 1	166 1	162 1.5	164 1.5	162 2	164 2	164 ev 2.5 Mev
1	3.87±0.04	4.40	4.24	4.17	4.19	4.12	4.08	4.01	3.89
2	11.59±0.06	11.72	11.66	11.62	11.65	11.61	11.61	11.57	11.52
3	22.18±0.06	22.18	22.18	22.18	22.18	22.18	22.18	22.18	22.18
4	35.55±0.10	35.55	35.58	35.62	35.57	35.62	35.62	35.67	35.70
5	51.64±0.15	51.65	51.70	51.79	51.68	51.77	51.76	51.85	51.93
6	70.31±0.20	70.36	70.42	70.57	70.37	70.52	70.49	70.64	70.74
12	233.2 ±0.7	233.2	233.1	233.7	232.8	233.4	233.1	233.8	233.9
15	345.0 ±1.0	345.0	344.7	345.6	344.2	345.1	344.6	345.4	345.7
18	476.0 ±1.3	475.7	475.3	476.4	474.6	475.1	475.0	476.1	476.5

[12] J. C. Slater, Phys. Rev. 98, 1039 (1955).

TABLE IX. Theoretical stopping power and range-energy relation for protons in Al with $I=163$ ev and $C_L=3.2\times10^{-3}\times\beta^2=1.5/E$ (Mev) above 1 Mev; see text for C_L below 1 Mev. C_K according to Walske.

E (Mev)	$\frac{1}{\rho}\frac{dE}{dt}$ (theor) (Mev/g cm^{-2})	R (theor) (mg cm^{-2})	$\frac{1}{\rho}\frac{dE}{dt}$ (exp) (a)	(b)	R (exp) (c)
0.1	371		416	425	
0.15	360		366	397	
0.2	343		334	368	
0.25	327		314	342	
0.3	310		293	320	
0.35	293		279	301	
0.4	279		268	284	
0.5	252		250	258	
0.6	230		233	237	
0.7	212		217	217	
0.8	197		202	202	
0.9	185		190	188	
1.0	173	4.15	177	176	3.87
1.2	155	5.38	154	157	5.16
1.4	141	6.74	135	142	6.59
1.6	129	8.23	123	123	8.14
1.8	119	9.85	117	120	9.82
2.0	111	11.60	112	112	11.59
3.0	83.2	22.15			22.18
4.0	67.6	35.56			35.55
5.0	57.3	51.70			51.64
6.0	50.0	70.42			70.31
7.0	44.5	91.64			
8.0	40.2	115.3			
9.0	36.8	141.3			
10.0	33.9	169.6			
12.0	29.5	233.1			233.2
14.0	26.1	305.3			
16.0	23.5	386.0			
18.0	21.5	475.1			476.0
20.0	19.8	572.3			

[a] See reference 14.
[b] See reference 15 (best fit curve).
[c] See reference 5 and this paper.

integration ϵ in Eq. (17) is as large as 2 Mev, the maximum in the L-shell correction will occur at an energy less than one-fifth of the lowest energy to which the stopping power formula is applied. Then we need not hesitate to use $C_L=\kappa/E$.

A number of theoretical range tables have been computed on this basis. Numerical values of the parameters used are: $\kappa=0$, 1, 1.5, 2, and 2.5 Mev; $I=160$, 162, 164, 166, and 168 ev. Computations were made with all possible combinations. The results for the most useful ones are listed in Table VIII. These values are adjusted so that $R(\epsilon)=22.18$ mg cm^{-2} for $\epsilon=3$ Mev.

The experimental ranges for Al as corrected for multiple scattering are also listed in Table VIII. Since the multiple scattering correction for Al is small, the values of ΔR_0 for each of the various energies are best determined theoretically using Eq. (6), and they have in fact been so determined. One then finds $\xi=4.4\pm0.4$ for protons of 5 to 20 Mev, and consequently from Table II $q=0.94$. Then $\Delta R_{\frac{1}{2}}=0.94\,\Delta R_0$. Adding $2\Delta R_0/15$ according to Eq. (16) the total multiple scattering correction is $\Delta R=1.07\,\Delta R_0$. These values have been added to the experimental ranges as given in reference 5 to give the corrected ranges as listed in Table VIII. For the case of Al which we are considering here, these corrections are barely equal to the errors of measurement but they introduce a systematic trend which is significant for the determination of stopping power and the parameters which appear in the stopping power relation. For Ni and Ag where the corrections would be larger, only preliminary data are available.[13]

The theory[1] of the L-shell correction predicts $\kappa\sim1.5$ Mev. Reference to Table VIII indicates that this choice of κ with $I=163$ ev is satisfactory for the entire range of energies above 2 Mev.

In an effort to extrapolate the calculations to somewhat lower energies the stopping power was calculated at energies below 1.5 Mev by using a modified C_L correction at these lower energies but still retaining $I=163$ ev. The C_L correction used is believed to be consistent with the prediction of the Walske theory[1] with $\theta_L=0.35$. The calculated stopping power and ranges are given in Table IX. For comparison we give also the stopping power as determined by Allison[14] and Whaling.[15] The theory appears satisfactory to 0.15 Mev for the explanation of the experimental stopping powers, but the disagreement between experimental and theoretical ranges is larger than the experimental errors below 1.8 Mev. For the ranges above 3 Mev a better fit is obtained with $I=166$ ev and $C_L=0$ (see Table VIII). At present this choice appears undesirable from a theoretical point of view. It will be interesting to see what the situation is in heavier elements in which the multiple scattering correction is larger and binding energy corrections for the M shell as well as for the K and L shells have to be taken into account.

[13] B. J. Farmer, thesis, The Rice Institute (unpublished), and Bull. Am. Phys. Soc. **5**, 263 (1960).
[14] S. K. Allison and S. D. Warshaw, Revs. Modern Phys. **25**, 779 (1953).
[15] W. Whaling, in *Encyclopedia of Physics* (Springer-Verlag, Berlin, 1958), Vol. 34, p. 202.